Performance Measurement of the Upgraded DØ Central Track Trigger

Remigius K. Mommsen

on behalf of the DØ CTT Group:

John Anderson[1], Robert Angstadt[1], Levan Babukhadia[2], Mrinmoy Bhattacharjee[2], Gerald Blazey[3], Oana Boeriu[4], Fred Borcherding[1], Marc Buehler[5], Brian Connolly[7], Michael Cooke[6], Marjorie Corcoran[6], Satish Desai[2], David Evans[8], Yuri Gershtein[9], Paul Grannis[2], Stefan Grünendahl[1], Liang Han[10], Eric Hazen[11], Ulrich Heintz[11], Carsten Hensel[12], Mike Hildreth[4], Hendrik Hoeth[13], Yuan Hu[2], Shabnam Jabeen[11], Vivek Jain[14], Marvin Johnson[1], Remigius K. Mommsen[16,1], Samvel Khalatian[11], Norik Khalatyan[11], Don Lincoln[1], Stephan Linn[7], Yanwen Liu[10], Juan Lizarazo[15], Dennis Mackin[6], Yurii Maravin[1], Manuel Martin[3], Yildirim Mutaf[2], Meenakshi Narain[11], Carsten Nöding[17], Jamieson Olsen[1], Paul Padley[6], Monica Pangilinan[11], Richard Partridge[9], Ricardo Ramirez-Gomez[15], Stefano Rapisarda[1], Kyle Stevenson[18], Makoto Tomoto[1], Brigitte Vachon[1], Thei Wijnen[19], Neal Wilcer[1], Graham Wilson[12], Shouxiang Wu[11], Terry Wyatt[16], Qichun Xu[20], Kin Yip[14]

Abstract— The DØ experiment was upgraded in spring 2006 to harvest the full physics potential of the Tevatron accelerator at Fermi National Accelerator Laboratory, Batavia, Illinois, USA. It is expected that the peak luminosity delivered by the accelerator will increase to over 300×10^{30} cm^{-2}s^{-1}. One of the upgraded systems is the Central Track Trigger (CTT). The CTT uses the Central Fiber Tracker (CFT) and Preshower detectors to identify central tracks with $p_T > 1.5$ GeV at the first trigger level. Track candidates are formed by comparing fiber hits to predefined track equations. In order to minimize latency, this operation is performed in parallel using combinatorial logic implemented in FPGAs. Limited hardware resources prevented the use of the full granularity of the CFT. This leads to a high fake track rate as the occupancy increases. In order to mitigate the problem, new track-finding hardware was designed and commissioned. We report on the upgrade and the improved performance of the CTT system.

Remigius K. Mommsen is with the School of Physics and Astronomy at the University of Manchester, Manchester, UK, and the Fermi National Accelerator Laboratory, Batavia, IL, USA (telephone: 630-840-8321, e-mail: mommsen@fnal.gov)

[1] Fermi National Accelerator Laboratory, Batavia, IL 60510, USA
[2] SUNY Stony Brook, Stony Brook, NY 11794, USA
[3] NICADD/NIU, Northern Illinois University, DeKalb, IL 60115, USA
[4] University of Notre Dame, Notre Dame, IN 46556, USA
[5] University of Virginia, Charlottesville, VA 22904, USA
[6] Rice University, TW Bonner Nuclear Lab, Houston, TX 77251, USA
[7] Florida State University, Tallahassee, FL 32306, USA
[8] Lancaster University, Lancaster LA1 4YW, United Kingdom
[9] Brown University, Providence, RI, USA
[10] University of Science and Technology of China, Hefei, China
[11] Boston University, Boston, MA 02215, USA
[12] University of Kansas, Lawrence, KS 66045, USA
[13] Bergische Universität Wuppertal, 42097 Wuppertal, Germany
[14] Brookhaven National Laboratory, Upton, NY 11973, USA
[15] Universidad de Los Andes, Bogota, Colombia
[16] University of Manchester, Manchester M13 9PL, United Kingdom
[17] Albert-Ludwigs-Universität Freiburg, 79005 Freiburg, Germany
[18] Indiana University, Bloomington, IN 47405, USA
[19] University of Nijmegen, 6546 ED Nijmegen, The Netherlands
[20] University of Michigan, Ann Arbor, MI 48109, USA

I. INTRODUCTION

THE DØ detector is located at the Tevatron accelerator at Fermi National Accelerator Laboratory, Batavia, Illinois, USA. [1], [2] The Tevatron accelerates protons and anti-protons to energies of about 1 TeV. Particle bunches are collided head-on in the center of the detector. Interactions between protons and anti-protons, or events, result in the production of elementary particles such as electrons, muons, quarks and gluons materialized as jets, photons, and neutrinos (inferred by missing transverse energy of an event). The Tevatron bunch crossing period is 396 ns. However, the CTT hardware is designed to support bunch crossing periods of 396 ns and 132 ns. The data bandwidth produced by all of the DØ readout electronics far exceeds what can be saved for offline storage and analysis. For this reason, a trigger system is needed to quickly analyze detector data and select only the interesting physics events. DØ utilizes three levels of triggers, each successive level incorporating more rigorous filter algorithms [3], [4]. Level 1 consists of custom hardware/firmware-based triggers that search for patterns consistent with electrons, muons, and jets. Level 2 relies on conventional CPUs and digital signal processors to combine first level objects and additional information of muons, electrons, and jets. Level 3 is a computer farm that uses software algorithms for particle identification after simple event reconstruction. The maximum allowable trigger rates for events passing level 1, 2, and 3 are about 10 kHz, 1.5 kHz, and 50 Hz, respectively.

II. THE CENTRAL TRACK TRIGGER

One of the main components of the DØ first level trigger is the Central Track Trigger (CTT) [5]. The CTT reconstructs trajectories of charged particles using fast discriminator data provided by Central Fiber Tracker (CFT). The CFT consists

CFT AXIAL LAYERS

one 4.5° sector
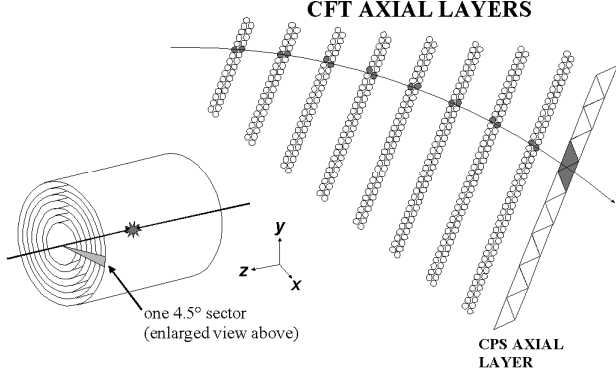(enlarged view above)

CPS AXIAL
LAYER

Fig. 1. Schematic view of the axial part of the Central Fiber Tracker (CFT). It consists of 8 concentric doublet layers of scintillating fibers and a pre-shower detector (CPS) surrounding the interaction point. One of the 80 4.5° sectors used by the CTT is shown with a hypothetical track overlaid.
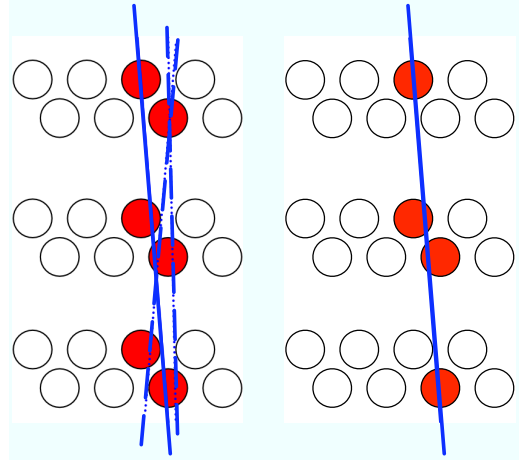

Fig. 2. Schematic view of 3 doublet layers. On the left, the doublet scheme is depicted, showing that beside the correct track (solid blue line) other tracks (dashed blue lines) can trigger the same equation. With the singlet equation shown on the right, only the correct track fires the trigger.

of 71,680 1 mm scintillating fibers mounted on eight carbon-composite cylinders at radii ranging from 20 to 52 cm. Approximately half of the CFT fibers are positioned axially (parallel to the beam line), while the rest are helically arranged at a small stereo angle. Each of the 8 axial and 8 stereo layers consists of a doublet layer of fibers shifted by about half a fiber width. The CFT cylinders are positioned inside of a super conducting solenoid magnet that produces a 2 Tesla magnetic field. The trajectory of a charged particle is bent in the transverse plane of the detector with a curvature inversely proportional to the transverse momentum p_T of the particle. The CFT provides coverage down to about 22° from the beam axis. The readout is segmented into 80 4.5°-wide sectors (figure 1).

The CTT forms track candidates in the $r - \phi$ plane by comparing fiber hits in the axial layers of the CFT to predefined track equations, using 4 different p_T thresholds of 1.5 GeV, 3 GeV, 5 GeV, and 10 GeV. The track origin has to be within a radius of 300 μm from the nominal beam spot. Each of the 80 sectors in ϕ is treated separately, taking into account that tracks might cross from one sector to the next. In addition, isolated tracks and tracks with matched pre-shower information are flagged accordingly. The CTT also delivers track candidates to the level 1 muon and CalTrack trigger. The latter combines calorimeter clusters with tracks to form electron and τ candidates. Furthermore, CTT track candidates are used to seed the track finding using the silicon tracker on the second trigger level.

In order to minimize latency, track finding is performed in parallel using combinatorial logic implemented in FPGAs. The original hardware limits the number of combinations (equations) to approximately 16,000 per sector. Therefore, the full granularity of the CFT needed to be reduced by combining adjacent fibers in the inner and outer layers of each doublet layer into one space point, leaving 8 points per track. This scheme has the disadvantage that the trigger rate increases non-

linearly with luminosity due to fake tracks (see figure 2). In order to cope with the increasing luminosity while keeping the same latency for track finding, new hardware using larger FPGAs was designed [6]. The increased FPGA capacity enables the use of single fiber hits to form tracks, employing about 50,000 equations per sector.

III. UPGRADE

The new track finding hardware was designed to seamlessly replace the old hardware, i.e. no modifications are required for any of the upstream or downstream systems. In order to certify the new hardware and firmware before the actual installation, the input into the track finding hardware for 4 out of the 80 sectors was split and fed into the new hardware running in parallel to the old system for more than one year. This provided an excellent test bed to assess the reliability of the new hardware, to gain operational experience in controlling and monitoring, and to evaluate new trigger algorithms. In the first phase of testing, the same algorithms as on the old system were used, allowing a direct cross-check of the physics performance. In later phases, different versions of trigger algorithms were deployed and compared to the old system. However, the comparison was somewhat hampered by the limited statistics obtained by looking only at 4 out of 80 trigger sectors. About 2 months before the upgrade, a partial implementation of the new algorithm was deployed on the old hardware. This allowed a direct measurement of the trigger rate reduction achievable and gave a credible cross-check of the simulation results. In addition, the reduced trigger rate enabled the experiment to record more physics events at steadily increasing luminosities.

The actual upgrade took place from March to May 2006. Together with the more powerful track-finding hardware, other improvements were implemented. For easier maintenance all cables are connected to the back of the crate (see figure 3). Failing boards can now be replaced without having to remove

the input cables as it was the case for the old system. The boards are programmed and controlled via a fast Gigabit Ethernet connection allowing for much faster downloads of new firmware as compared to the old boards which were controlled by a serial 1553 bus. In addition, the power distribution to the boards is improved by using redundant 48 V DC power supplies with on-board voltage regulators.

The commissioning of the upgraded system in June 2006 proceeded smoothly. The system was operational well before the first beam arrived, enabling the experiment to trigger on cosmic ray events. This allowed to check out the trigger system and provided alignment information for the whole detector. After Tevatron operation resumed, the same doublet equations were loaded as used before the shut-down. This enabled the direct comparison of the physics performance between the new and old system. After this initial certification period, singlet equations were loaded, yielding a much better performance of the CTT.

IV. PERFORMANCE

One of main worries for a track trigger is the ability to efficiently trigger on tracks while the occupancy of the CFT increased due to higher luminosities. Current plans are to increase the peak luminosity from $200 \times 10^{30} \, \mathrm{cm}^{-2}\mathrm{s}^{-1}$ to above $300 \times 10^{30} \, \mathrm{cm}^{-2}\mathrm{s}^{-1}$ within the next year.

Figure 4 shows the trigger rates for single and double track triggers using the four different p_T thresholds as a function of luminosity. The trigger rate is reduced by a factor up to 4 (10) for the single (double) track trigger based on singlet equations. However, further improvements to the trigger algorithms will need to be implemented to cope with the highest expected luminosities [7].

One figure of merit for a track trigger is the track finding efficiency vs the p_T of the track. The efficiency is defined as the ratio of the number of tracks found online to the number of matched offline reconstructed tracks. An offline track is required to be within the acceptance of the CFT detector, to produce light in all 16 stereo and axial CFT layers, to originate from within $100 \, \mu\mathrm{m}$ of the primary vertex, and to have a fit $\chi^2 < 5$. Only tracks from events which have not been triggered by the CTT are considered. The offline track is matched in ϕ and p_T to the track candidates found by the CTT.

Ideally, the trigger efficiency should be 1 for tracks above the p_T threshold, and 0 below. Figure 5 compares single track trigger turn-on curves for doublet and singlet equations. The singlet equations provide a sharper turn-on with reduced contributions from tracks below the p_T threshold as compared to the doublet equations. The plateau efficiency is similar in both cases.

Another possibility to quantify the trigger efficiency is to look at muons from $Z^0 \rightarrow \mu^+\mu^-$ decays. We study events where one of the muons was triggered by the single muon trigger without the use of a CTT track. The other muon is then used to probe if the CTT has fired. In order to quickly assess the performance of different equation sets, the raw data of these

events are fed into a simulation of the CTT hardware. Due to the limited number of available events for this study, the efficiency is calculated for 5 super-sectors, which are shifted by $-36°$ in ϕ compared to the numbering of the trigger sectors. Figure 6 shows the efficiency of the probe muon to fire the single track trigger for $p_T > 10 \, \mathrm{GeV}$ using the doublet and singlet equation sets, respectively. Sectors $72-7$ show an additional inefficiency for the doublet equations, which is unrelated to the upgrade of the CTT. It is partially attributed to an improved representation of the CFT geometry used for generating the equations. Overall, we find that the efficiency for the singlet equations is higher.

V. CONCLUSIONS

The first level central track trigger of DØ was upgraded to exploit the full granularity of the central fiber tracker. The upgraded trigger was ready in time. The trigger rates for single (double) track triggers are reduced by a factor of up to 4 (10). The track finding efficiency is similar or even better as compared to with the old system. In addition, the trigger turn-on curves became sharper. However, the envisaged increase of the peak luminosity to above $300 \times 10^{30} \, \mathrm{cm}^{-2}\mathrm{s}^{-1}$ will need further improvements to the track finding algorithms to exploit the full physics potential of DØ.

REFERENCES

[1] S. Abachi *et al.*, "The D0 Detector," *Nucl. Instrum. Meth.*, vol. A338, pp. 185–253, 1994.
[2] V. M. Abazov *et al.*, "The upgraded d0 detector," *Nucl. Instrum. Meth.*, vol. A565, pp. 463–537, 2006.
[3] G. C. Blazey, "The DØ run II trigger," 1997, to be published in the proceedings of 10th IEEE Real-Time Computer Applications in Nuclear, Particle and Plasma Physics (RT 97), Beaune, France, 22-26 Sep 1997.
[4] R. Schwienhorst, "The DØ Run II trigger system," *Int. J. Mod. Phys.*, vol. A20, pp. 3796–3798, 2005.
[5] J. Anderson *et al.*, "The DØ Central Track Trigger," *IEEE Trans. Nucl. Sci.*, vol. 51, pp. 345–350, 2004.
[6] E. Hazen *et al.*, "Hardware Aspects of the Upgraded DØ Central Track Trigger," in these proceedings.
[7] G. Wilson *et al.*, "Trigger Algorithms, Simulation and Performance Optimization of the DØ Central Track Trigger," in these proceedings.
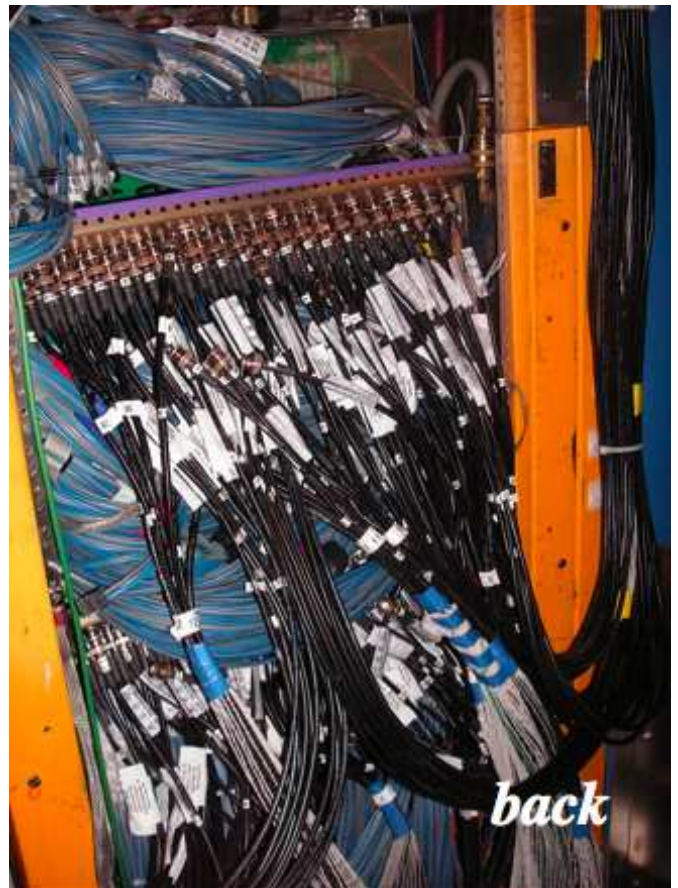
Fig. 3. The new track finding hardware installed under the DØ detector. The 40 new DFEA2 boards are arranged in 2 crates, easily accessible from the front. The 320 input and 320 output cables are located in the back of the crates.
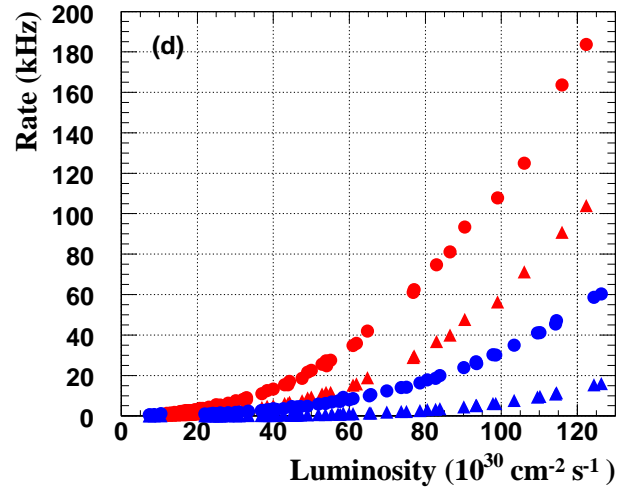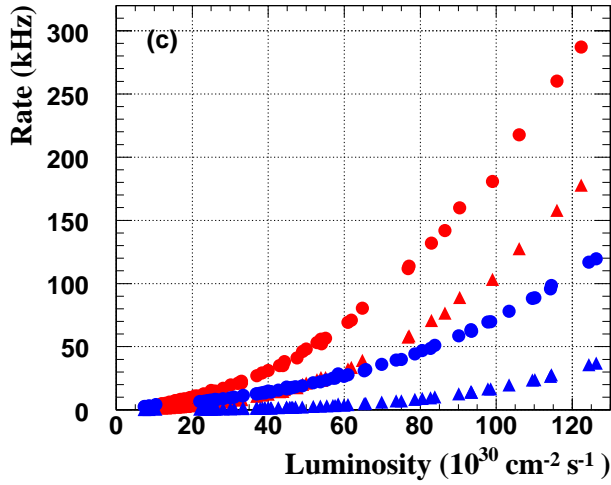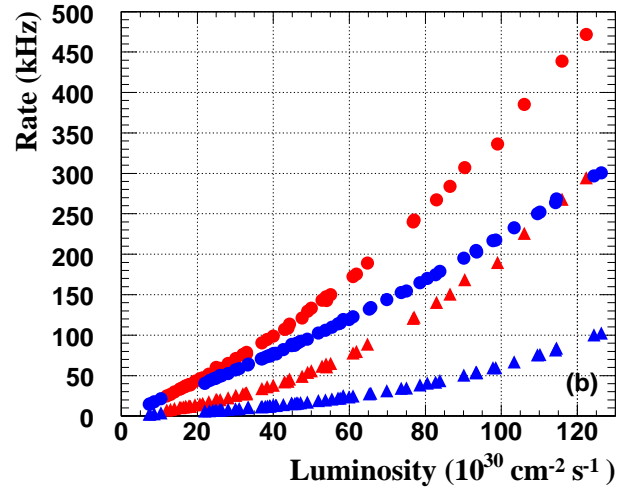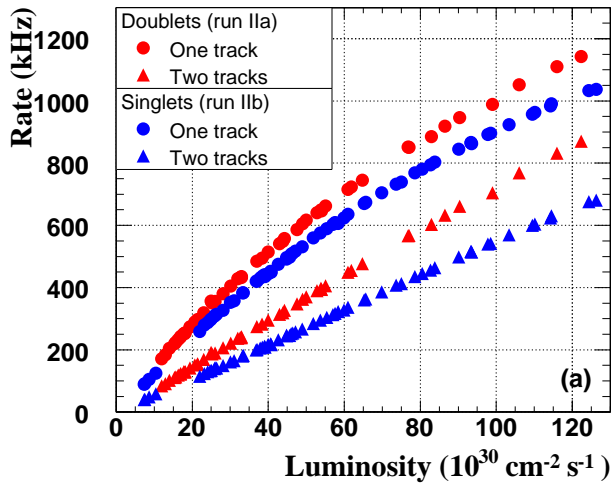
Fig. 4. Level 1 trigger rates for the single and double track triggers as a function of luminosity for doublet equations (red) and singlet equations (blue) using the four different p_T thresholds of 1.5 GeV (a), 3 GeV (b), 5 GeV (c), and 10 GeV (d).
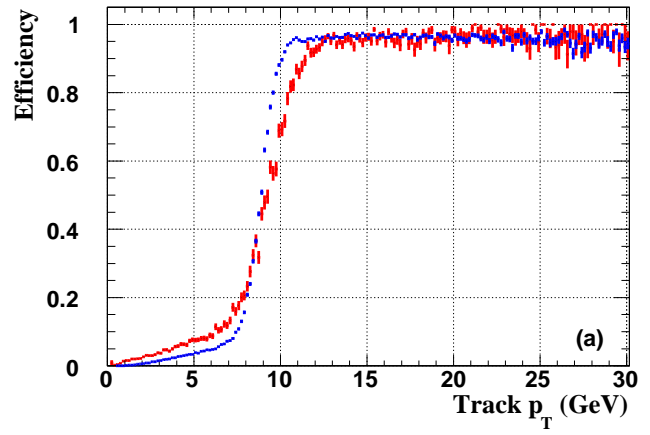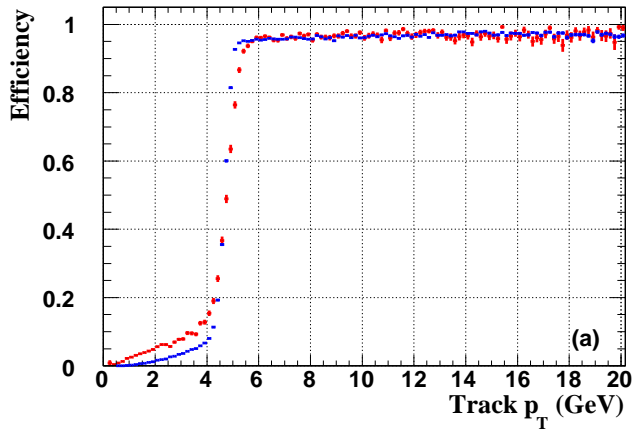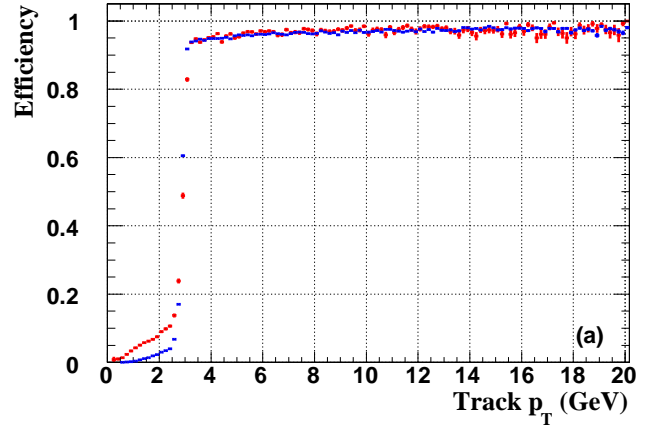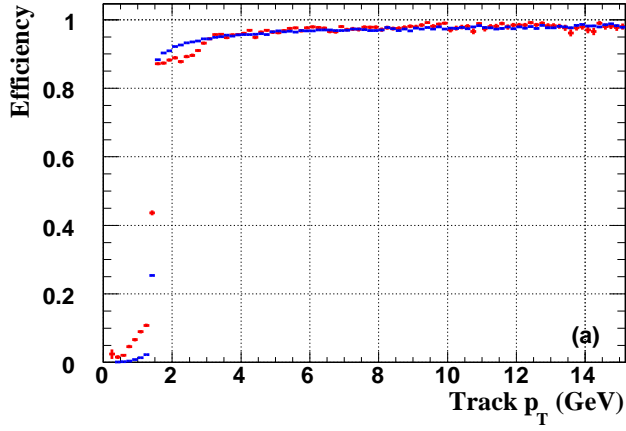
Fig. 5. Single track trigger turn-on curves for doublet equations (red) and singlet equations (blue) for the 4 different p_T thresholds of 1.5 GeV (a), 3 GeV (b), 5 GeV (c), and 10 GeV (d).
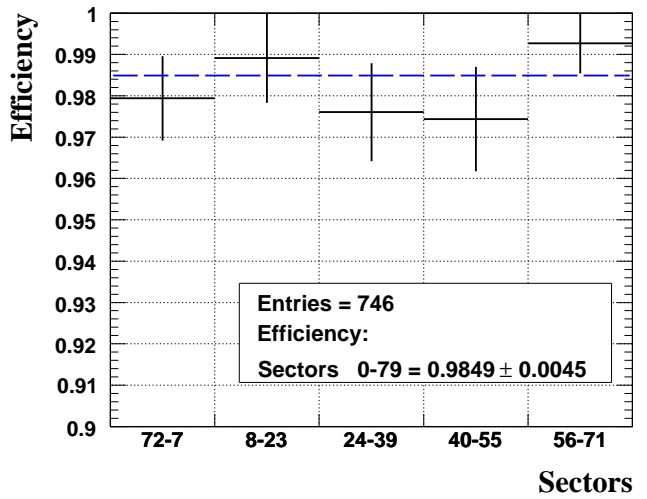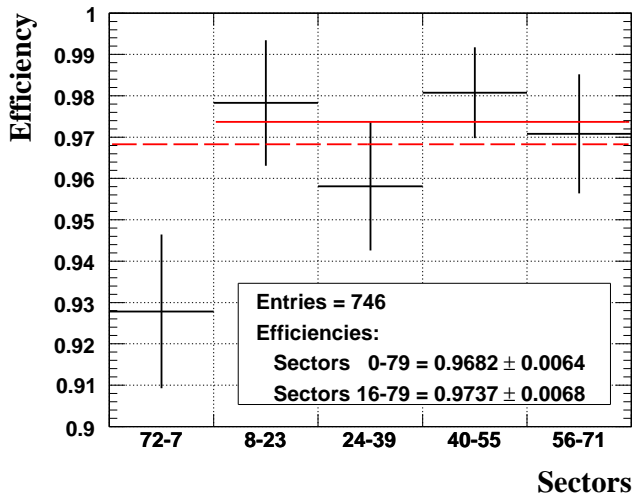

Fig. 6. Single track trigger efficiencies for tracks with $p_T > 10$ GeV determined for muons from $Z^0 \rightarrow \mu^+\mu^-$ decays. Left (right) for doublet (singlet) equations.